

Crystal Engineering to Avoid Pairing Dipolar Moments: The Case of 5-Nitouracil, a Highly Polarizable Molecule

Manuela Ramos Silva * and Pedro Pereira da Silva

CFisUC, Physics Department, University of Coimbra, P-3004-516 Coimbra, Portugal

* Correspondence: manuela@uc.pt

Abstract: 5-nitouracil is a polarizable molecule with a permanent electric dipole moment. Its molecular properties caught the attention of physicists working on nonlinear optics or optoelectronics, but the translation of the molecular assets to the crystalline solid has not been straightforward. This review compares all the known crystal structures incorporating the neutral or ionic 5-nitouracil, or the two species concomitantly, discussing the effect of the packing in the optimization of the crystalline optical properties. Two new centrosymmetric 5-nitouracilate salts are also reported for the first time, showing extensive hydrogen bonding between anions and cations. This review also gathers data from nonlinear optical measurements of non-centrosymmetric crystals and thermal stabilities of known polymorphs, showing that a neutral 5-nitouracil molecule in acentric crystalline environment allows efficient blue-light generation.

Keywords: 5-nitouracil; dipolar moment; crystal engineering; supramolecular interaction; hydrogen bond; non-linear optics

Citation: Ramos Silva, M.; Pereira da Silva, P. Crystal Engineering to Avoid Pairing Dipolar Moments: The Case of 5-Nitouracil, a Highly Polarizable Molecule. *Crystals* **2023**, *13*, 145. <https://doi.org/10.3390/cryst13010145>

Academic Editor: Manuela E. Crisan, Lilia Croitor and Roxana Popescu

Received: 6 December 2022

Revised: 27 December 2022

Accepted: 1 January 2023

Published: 13 January 2023



Copyright: © 2023 by the authors. Licensee MDPI, Basel, Switzerland. This article is an open access article distributed under the terms and conditions of the Creative Commons Attribution (CC BY) license (<https://creativecommons.org/licenses/by/4.0/>).

1. Introduction

In 1961, P. Franken et al., at the University of Michigan, focused a pulsed ruby laser ($\lambda = 694$ nm) into a quartz crystal. Using 3 *joules* of energy in the red pulse, they generated a few *nanojoules* of blue light ($\lambda = 347$ nm) [1]. This experiment sets the birth of Nonlinear Optics. When Nonlinear Optical (NLO) materials are subjected to intense laser light, dramatic changes may occur in the frequency, phase and polarization of the incoming light.

The nonlinear interaction between the electromagnetic field of the light and of the charge distribution of the crystal originates several phenomena including frequency-mixing processes, such as second-harmonic generation (SHG) (or frequency doubling, generation of light with a doubled frequency—half the wavelength) and third-harmonic generation (THG) (generation of light with a tripled frequency—one-third the wavelength) [2]. It is the second-harmonic generation that allows the expansion of the laser's spectra up to the ultraviolet, using inorganic crystals such as KTiOPO_4 or LiNbO_3 , well-established commercially available materials.

However, non-linearity can also be found in organic compounds such as Rentzepis and Pao, from the Bell laboratories, showed in 1964, by making the first observation of SHG in an organic material, namely in benzopyrene and benzanthracene [3]. Foreseeing applications in optical devices, SHG organic crystals have to provide high SHG efficiency, high transparency, adequate birefringence to allow phase-matching and high damage threshold. The materials should also be easy to grow into large single crystals and be chemical and physical stable [4].

An approach that has been proven successful to obtain high NLO responses is the use of molecules with high dipolar moments [5,6], namely, push–pull organic chromophores, molecules consisting of an electron donor (D) group and an electron-withdrawing (A) group connected via a π -conjugated organic backbone. Para-nitroaniline is the

archetypal model of a D- π -A chromophore: NH₂ is the donor group, NO₂ is the acceptor group both substituted across an aromatic benzene ring. It shows an exceptionally strong charge-transfer character associated with a large polarizability and hyperpolarizability [7–9]. However, exceptional molecular properties do not often translate into the crystalline form; the polar nature of the push-pull chromophores leads to a tendency to self-assemble in centrosymmetric structures driven by dipole-dipole interactions, hindering their applicability [10].

How can we circumvent such tendency?

One way is to incorporate dipolar chromophores into a polymer host [11] and apply a strong electric field while heating and cooling (electric field poling). The NLO chromophores show a preferential orientation along the field direction [12]. Another approach is a controlled crystallization, using counter-ions or co-formers that induce an acentric assembling. Single crystals provide a high degree of ordering as well as a large concentration of chromophores per unit volume and, by using birefringence, phase matching can be achieved [13].

The relation between the macroscopic and the molecular optical response is not straightforward because of interactions between neighboring molecules. However, in a first approximation, the bulk response can be explained by the so called oriented-gas model: molecules are considered to be frozen and non-interacting and an additivity approach is used to account for the crystal nonlinearities [14]. Zyss and Oudar, in 1982 [15], perfected the model by considering the mutual polarization effects of neighboring molecules as local-field corrections. For compounds in which molecules/ions interactions are too strong to be considered a correction, a supermolecule approach can be used. In this approach a cluster containing the main intermolecular interactions takes the role of a single molecule in the oriented gas model [16]. When calculating the macroscopic susceptibility from the molecular/supermolecular hyperpolarizability tensor, one often has also to consider the transformation of molecular reference frame to the crystal reference frame, to consider the symmetry of the molecular assembling and even further simplifying symmetry conditions (like the Kleinman symmetry—all three indices in the hyperpolarizability tensor are universally interchangeable [17]).

Jerphagnon, in 1971, was the first to note that a crystalline form of 5-nitrouracil showed a NLO response comparable to that of the inorganic barium-sodium niobate [18].

5-nitrouracil (5NU) can be considered a cyclic urea derivative, with a strong electron-accepting group (the nitro group), see Figure 1. Further optical studies were presented in conferences in the eighties, but it was Zyss and co-workers that performed a thorough study of the acentric form of 5NU, reporting in 1993 [19] the efficient non-linear response of 5NU; it permits efficient blue-light generation from a pulsed, 1.34-mm Nd³⁺:YAG laser.

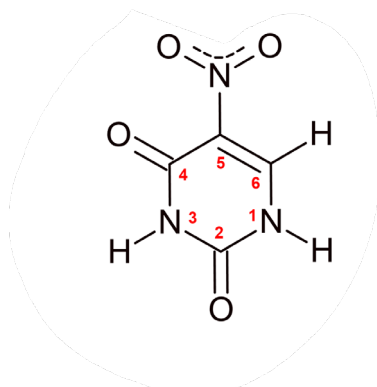


Figure 1. Schematic molecular structure of 5NU with numbering convention.

Zyss and co-workers reported that 5NU exhibits a transparency interval of circa 1000 nm, a nonlinear optical coefficient of 8.7 pm/V, a laser damage threshold (limit at which a

material will be damaged by a laser given the power per area) of 3 GW/cm² (at 1.06 μm wavelength, pulse duration ~10 ns). Phase matching is also observed with narrow angular acceptance. Furthermore, 5-Nitouracil crystals show excellent optical quality and can be grown by a thermal-gradient transport method based on natural convection. The crystals exhibit excellent air conservation. Table 1 shows a comparison of 5NU with some well-known mineral and organic crystals [19] sanctioning 5NU as one of the best nonlinear organic crystals.

Table 1. Comparison of 5NU with some well-known mineral and organic crystals; adapted with permission from Ref. [19], 1993, Optica Publishing Group.

| Compound | LiNbO ₃ [20,21] | KTiOPO ₄ [22,23] | Urea [24,25] | POM [26] 3-Methyl-4-nitro-pyridine-1-oxide | 5NU [19] |
|---|---|--|--|---|--|
| Transparency range (nm) | 330–6000 | 350–4500 | 230–1440 | 450–1550 | 410–1550 |
| Symmetry Class | Trigonal 3m | Orthorhombic mm2 | Tetragonal 42m | Orthorhombic 222 | Orthorhombic 222 |
| Nonlinear-optical coefficients (at 1.06 μm) | $d_{15} = 4.4$ pm/V $d_{22} = 3.6$ pm/V $d_{33} = -47$ pm/V | $d_{31} = 6.5$ pm/V $d_{32} = 5.0$ pm/V $d_{33} = 13.7$ pm/V $d_{15} = 6.5$ pm/V $d_{33} = 7.6$ pm/V | $d_{14} = 1.4$ pm/V | $d_{14} = 10$ pm/V | $d_{14} = 8.7$ pm/V |
| Damage threshold | (40 ns) 0.69, >1 GW/cm ² | (1 ns) 1.06, 15 GW/cm ² | (10 ns) 1.06, 0.355, 30 MW/cm ² | (10 ns) 1.06, 200 MW/cm ² 0.532, 20 MW/cm ² | (10 ns) 1.06, 3 GW/cm ² 0.532, 1 GW/cm ² |
| Growth Technique | Czochralski method $T_m = 1260$ °C | Temperature gradient transport | Temperature variation $T_m = 135$ °C | Temperature variation $T_m = 136$ °C | Temperature gradient transport |
| Some remarkable properties | Good air conservation | Excellent air conservation | Hygroscopic | Closed cell with index liquid | Excellent air conservation |

Besides the NLO physics community, 5NU also has relevance to the biological and pharmaceutical sciences [27–29], reported for example as an active chemotherapeutic and mutagenic agent [30,31]. Its derivatives have shown antibacterial activity, antitumor activity on leukemia cells and inhibitory effects on macrophage [32].

At present, three crystalline forms of 5NU are known, two centric and one acentric. Several other co-crystals, salts and solvates have also been studied. This review is organized as follows: a brief section with the essential theoretical background; a succinct section for methods used in structure determination and ab-initio calculations; a description and comparison of structural feature of 5NU polymorphs with an emphasis on the acentric, second-harmonic generator; a description of co-crystals and solvates containing the 5NU neutral form; a discussion of L-histidinium 5-nitouracilate, a charge transfer transparent compound; a description of guanidine derivatives 5NU, including two new structures; and a description of other 5NU salts. In the conclusion section, we explore the lessons learned by the collection of 5NU compounds, that have been reported in the literature and reviewed in this paper.

2. Theoretical Background

There are excellent textbooks on nonlinear optics to which the reader is referred if he/she wants to dive deeper into the field [2,33]. We will briefly outline some concepts for the reader to follow.

In the case of conventional (i.e., linear) optics, the induced polarization, $\mathbf{P}(t)$ (electric dipole moment per unit volume), depends linearly on the electric field strength $\mathbf{E}(t)$ in a manner that can often be described by the relationship:

$$\mathbf{P}(t) = \epsilon_0 \chi^{(1)} \mathbf{E}(t) \quad (1)$$

where the constant of proportionality $\chi^{(1)}$ is known as the linear susceptibility and ϵ_0 is the permittivity of free space. For nonlinear optical phenomena, polarization is conveniently expressed as a sum of a linear term and nonlinear terms (Taylor series expansion of the dielectric polarization density $\mathbf{P}(t)$ at time t in terms of an electric field $\mathbf{E}(t)$ varying in time and space):

$$\mathbf{P}(t) = \mathbf{P}_l(t) + \mathbf{P}_{nl}(t) = \epsilon_0 (\chi^{(1)} \mathbf{E}(t) + \chi^{(2)} \mathbf{E}^2(t) + \chi^{(3)} \mathbf{E}^3(t) + \dots) \quad (2)$$

The quantities $\chi^{(2)}$ and $\chi^{(3)}$ are known as the second- and third-order nonlinear optical susceptibilities, respectively. In general, $\chi^{(n)}$ is an $(n+1)$ -th-rank tensor representing both the polarization-dependent nature of the interaction and the symmetries of the nonlinear solid.

Using Maxwell's equations and linear refractive index $n^2(\omega) = 1 + \chi^{(1)}$, one can write:

$$-\nabla^2 \mathbf{E}(r, t) + \frac{n(\omega)^2}{c^2} \frac{\partial^2 \mathbf{E}(r, t)}{\partial t^2} = -\mu_0 \frac{\partial^2 \mathbf{P}_{nl}(r, t)}{\partial t^2} \quad (3)$$

Some (anisotropic) materials have a refractive index that depends on the polarization and propagation direction of the light. These are called birefringent.

The microscopic polarization corresponds to the induced dipole moment which can be expanded as function of applied electric field:

$$\boldsymbol{\mu} = \boldsymbol{\mu}_0 + \alpha \mathbf{E} + \frac{1}{2!} \beta \mathbf{E}^2 + \frac{1}{3!} \gamma \mathbf{E}^3 \quad (4)$$

where $\boldsymbol{\mu}_0$ is the permanent dipole moment of the molecule. The coefficients α , β and γ are the linear polarizability, second-order nonlinear polarizability (or first hyperpolarizability) and third-order nonlinear polarizability (or second hyperpolarizability), respectively.

The first hyperpolarizability, β , is proportional to the difference between the ground and excited state dipole moments. Going from the molecular properties to the solid response, one has to consider the symmetry of the environment where the molecules/ions are placed and the effect of the environment on the molecular charge distribution. The mathematical relationship is:

$$d_{IJK} = \frac{1}{2} \chi_{IJK}^{(2)} = \frac{N}{V} f_I f_J f_K \frac{1}{N_g} \sum_s \sum_{ijk} \cos \theta_{ii}^{(s)} \cos \theta_{jj}^{(s)} \cos \theta_{kk}^{(s)} \times \beta_{ijk}^{(s)} \quad (5)$$

where I, J, K are the crystal axes, N_g is the number of equivalent positions in the unit cell of volume V that has N molecules (or supermolecules), $f_i(\omega)$ are local field factors for each crystal axis I , and the cosine product terms represent the transformation from the molecular reference frame to the crystal frame. The equivalent positions are labeled by the index s . The local field factors are essentially a correction for the difference between an applied field that would be felt by the molecule (or supermolecule) in vacuum and the local field within the solid.

The symmetry of the crystal reduces substantially the non-zero elements of the d_{IJK} array. For instance, for the 222 symmetry the array of nonlinear coefficients is reduced to:

$$\begin{pmatrix} 0 & 0 & 0 & d_{14} & 0 & 0 \\ 0 & 0 & 0 & 0 & d_{25} & 0 \\ 0 & 0 & 0 & 0 & 0 & d_{36} \end{pmatrix} \quad (6)$$

The components of the polarization vector are easily related to the electric field components:

$$\begin{cases} P_x = 2d_{14}E_yE_z \\ P_y = 2d_{25}E_xE_z \\ P_z = 2d_{36}E_xE_y \end{cases} \quad (7)$$

Further symmetry conditions, such as the Kleinman symmetry [17] conditions (valid when the applied frequencies are much smaller than any resonant frequencies and that assures interchangeability of all n indices in the rank n tensor describing the macroscopic nonlinear polarizability of a system) impose that $d_{14} = d_{25} = d_{36}$.

3. Materials and Methods

3.1. Synthesis

Guanidinium 5-nitrouacilate monohydrate: Guanidine carbonate (Aldrich 99%, 0.5 mmol) and 5-nitrouacil (Aldrich, 98%, 1 mmol) were dissolved in 100 mL of boiling water. The solution was left to evaporate under ambient temperature and pressure. Colorless prismatic single crystals grew from the solution by slow evaporation over a period of a few weeks.

Phenylguanidinium 5-nitrouacilate monohydrate: Phenylguanidine carbonate (Aldrich 99%, 0.5 mmol) and 5-nitrouacil (Aldrich, 98%, 1 mmol) were dissolved in 80 mL of boiling water. Small transparent and yellow crystals were deposited after a few weeks.

3.2. Structure Determination

For the determination of crystal structure by X-ray diffraction, small single crystals were glued to a glass fiber and mounted on a Bruker APEX II diffractometer. Diffraction data was collected at room temperature 293(2) K using monochromated MoK α ($\lambda = 0.71073$ Å). Absorption corrections were made using SADABS [34]. The structure was solved by direct methods using SHELXS-97 [35] and refined anisotropically (non-H atoms) by full-matrix least-squares on F^2 using the SHELXL-97 program [35]. The H positions of the NH₂ groups of the guanidinium ion were refined using the shelxl instruction HFIX 93. PLATON [36] and Mercury [37] were used for visualization and analysis of the structure. Atomic coordinates, thermal parameters and bond lengths and angles have been deposited at the Cambridge Crystallographic Data Centre (CCDC). Any request to the CCDC for this material should quote the full literature citation and the reference number CCDC 2222685–2222686.

3.3. Theoretical Methods

The calculation of the permanent dipole moment of the 5NU-5NU⁻ pair was performed with the GAMESS US package [38] within Density Functional Theory (DFT) using the Range-separated functional CAM-B3LYP [39] (Coulomb attenuated B3LYP with 19% HF plus 81% B88 exchange interaction at short-range, and 65% HF plus 35% B88 at long-range, with the intermediate region smoothly described through the standard error function with parameter 0.33) and the 6-311++G(d,p) basis set.

4. Results and Discussion

In this section, we review the structures containing the molecule of 5-nitrouacil or of its mononegative ion, along with the observed optical properties. We also present two new salts of 5NU. The following figures, Figures 2 and 3, portray the most common H-

bonded clusters between neutral 5-nitouracil and negative 5-nitouracil molecules. The approximate direction of the molecular dipolar moment is shown as a green arrow.

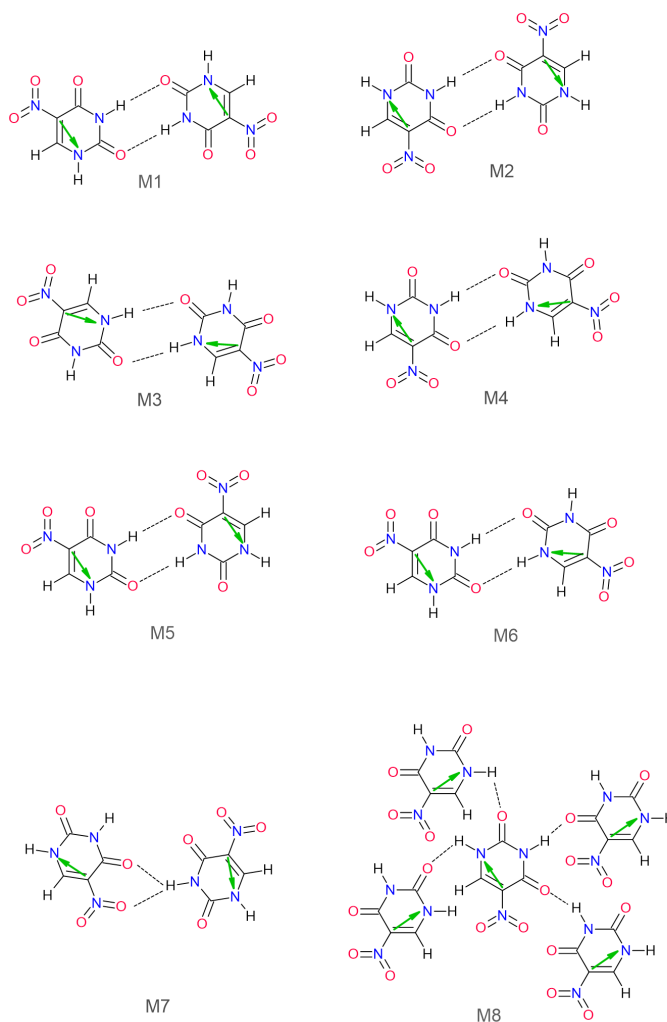


Figure 2. Typical H-bonding schemes with the neutral 5NU, the green arrows represent the dipole moment.

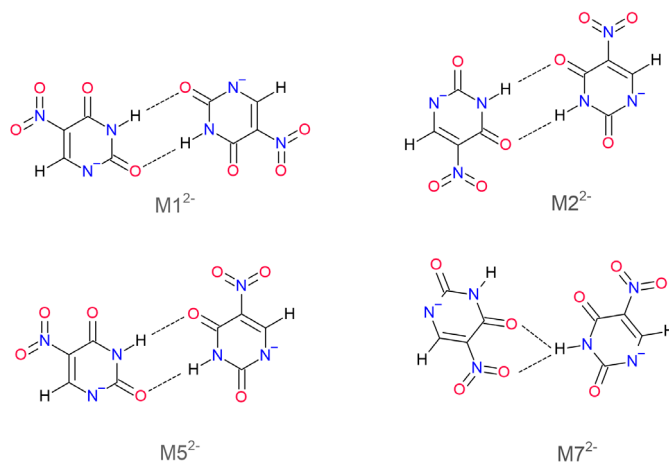


Figure 3. Typical H-bonding schemes with the negative ion, 5NU⁻. The same tags of Figure 2 were used for equivalent bonding schemes, for easy comparison, adding the overall charge in superscript.

4.1. Neutral 5NU

4.1.1. Polymorphs of 5NU

There are three known polymorphs of 5-nitrouracil: two centric and one acentric. Table 1 contains the main crystallographic information about the three crystal forms. In the two centric forms ($P2_1/n$ and $Pbca$), the molecules aggregate via H-bonds in chains. Within the chains we can see the M2 and M3 motif, with the dipolar moments anti aligning within the chain (Figure 4). Using Margaret Etter's [40–42] set of rules to describe hydrogen bonds, a first level graph sets rings with graph set symbol $R_2^2(8)$ for both M2 and M3 motif (in Etter's methodology the repeating hydrogen-bonding motifs are designated by descriptors with the general symbolization $G_a^d(n)$ where G indicates the motif, such as rings (R), chains (C), intramolecular (S) and discrete (D); a and d represent the number of acceptors and donors and (n) the number of atoms contained within the motif).

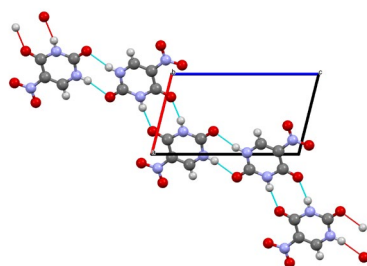
The crystal structures of **(I)** and **(II)** differ only slightly in the crystal packing of the chains.

Compound **(III)** is the acentric form of 5-nitrouracil. Molecules assemble in layers with an extensive H-bond network, parallel to the bc plane, in which each molecule bonds to four other molecules (Figure 5), and the first-level graph set symbol is C(4).

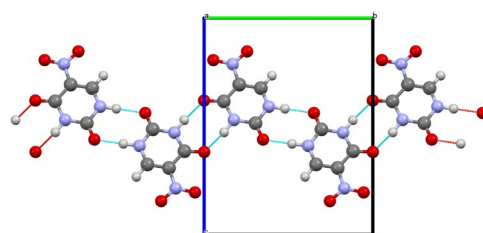
In the three polymorphs, the asymmetric unit comprises a whole molecule: the intramolecular geometry is essentially the same in the crystal structures and the molecule is nearly planar with the angle between the nitro group plane and the ring plane reaching 7° in compound **I** (Table 2).

Table 2. Crystallographic data of 5NU polymorphs.

| Compound/ CCDC Code | Unit Cell (Å, Å ³) | Space Group | Dihedral Angle between NO ₂ and Ring (°) | H-Bond Motif | Reference |
|---|---|----------------|---|--|-----------|
| 5-nitrouracil (I) NIMFOE | a = 5.873(1) b = 9.693(1) c = 10.4561(9) β = 104.07(1) V = 577.4(1) | $P2_1/n$ | 6.95(16) | Chains with alternating M2, M3 motifs | [43] |
| 5-nitrouracil (II) NIMFOE01 | a = 8.308(3) b = 10.426(3) c = 13.363(4) V = 1157.5(6) | $Pbca$ | 1.71(12) | Chains with alternating M2, M3 motifs | [44] |
| 5-nitrouracil (III) NIMFOE02 | a = 5.43420(10) b = 9.84060(10) c = 10.36590(10) V = 554.325(13) | $P2_12_12_1$ | 2.01(14) | Layers with M8 motif | [44] |



(a)



(b)

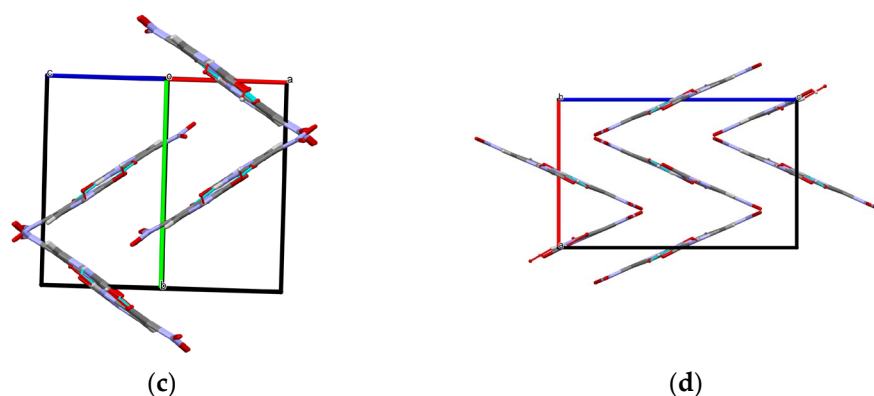


Figure 4. (a) H-bonded chain in (I). (b) H-bonded chain in (II). (c) Chain packing in (I). (d) Chain packing in (II).

Rao and co-workers [44] report in 2000 a charge density study of polymorphic forms II and III. They have calculated dipole moment vectors from the charge density distribution, obtained from X-ray diffraction data measured at low temperatures and processed with XD (a program that employs the multipolar atom model for determination, representation, and the property analysis of electron densities in crystal structures [45]). The approximated direction of such moments is shown in Figure 2, as green arrows, for the reader to quickly grasp the extinction or strengthening of the overall moment in the molecular clusters. Rao and co-workers have also calculated the molecular dipoles using a semi-empirical method for the quantum calculation of molecular electronic structures, Austin Model 1, or AM1 implemented in MOPAC [46]. They have used atomic coordinates directly taken from the experimental X-ray results and obtained similar magnitudes and directions for the dipole moments (circa 6 *Debye*, see Figure 2) of molecules in the centric (II) and acentric (III) form. Experimental values for the two forms, however, differ significantly. Experimental dipole values for the centric form coincide with the calculated ones, indicating that the effect of the environment is small in the molecular dipole moment. It is the assembling of the moments in a centric form that will reduce the moment of a unit cell to zero. Experimental dipole values for the acentric form differ from the calculated ones, indicating that the effect of an asymmetric crystal field in a noncentric structure can significantly enhance the dipole moment of each molecule. Furthermore, the vectorial summation of the moments will yield a large unit cell moment.

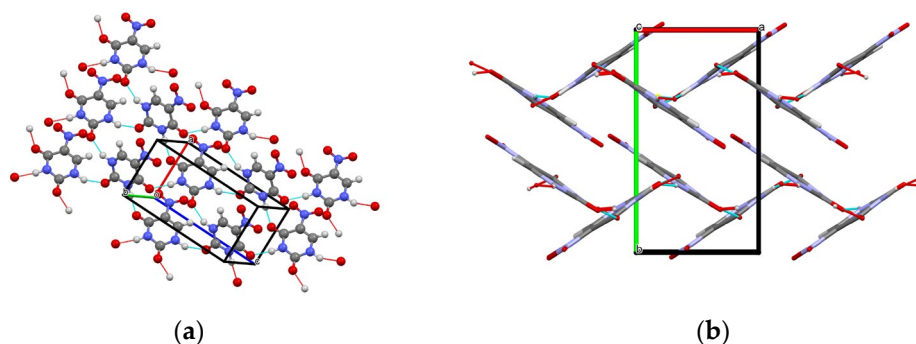


Figure 5. (a) H-bonded layer in (III). (b) H-bonded layer seen along the *c* axis in (III).

5-nitouracil single crystals in form (III) can be easily grown [19,47] from acetonitrile and show remarkable NLO properties that can compare to the inorganic counterparts (see Table 1). When form (III) is added to a saturated aqueous solution it dissolves. Moreover, following the thermal behavior of (III) one finds that it transforms into (I) at 252 °C [47].

4.1.2. 5NU Hydrates

There are two known water solvates of 5-nitrouracil. One form was first reported by Craven in 1967 (compound **IVa** [48]) and more recently re-determined at 120 K by Okoth et al. (**IVb** [47]); the second form was reported by us in 2008 (compound **V** [49]), see Table 3.

Table 3. Crystallographic data of 5NU monohydrates.

| Compound/ CCDC Code | Unit Cell (Å, °, Å ³) | Space Group | Dihedral Angle between NO ₂ and Ring (°) | H-Bond Motif | Reference |
|---|---|-------------------------|---|--------------------------|-----------|
| 5-nitrouracil monohydrate (IVa) NURAMH | <i>Reported:</i> a = 5.137(5) b = 21.956(6) c = 9.587(7) β = 143.50(8) V = 642 | <i>P2₁/c</i> | 4.96 ¹ | Layers with M2 motif | [48] |
| | <i>Conventional:</i> a = 5.137 b = 21.956 c = 6.254 β = 114.24 V = 643 | | | | |
| 5-nitrouracil monohydrate (IVb) NURAMH02 120 K | a = 5.06420(10) b = 21.9255(5) c = 6.11760(10) β = 113.1080(10) V = 624.77(2) | <i>P2₁/c</i> | 4.65(16) | Layers with M2 motif | [47] |
| 5-nitrouracil monohydrate (V) NURAMH01 | a = 6.27990(10) b = 7.8481(2) c = 13.8068(3) β = 93.8420(10) V = 678.94(3) | <i>P2₁/c</i> | 12.51(14) | 3D network with M1 motif | [49] |

¹Deposited coordinates do not contain uncertainty information.

In (**IV**), molecules of 5-nitrouracil are hydrogen bonded (N-H...O) in pairs across crystallographic centers of symmetry with the M2 motif (see Figures 2 and 6a). The resulting dimers are further hydrogen bonded through water molecules in layers parallel to the (10 $\bar{2}$) plane (conventional unit cell), at an interplanar separation of 2.979 Å [47]. In (**V**) the formation of pairs across crystallographic centers of symmetry is also seen, this time displaying the M1 motif (*R*²₂(8)). The dimers are interconnected through H-bonds involving the water molecules, forming a three-dimensional network (Figure 6b, [49]). In this form, the nitro group is rotated by 12.4(1)° out of the uracil plane, while in (**IV**) this rotation is less than 5°.

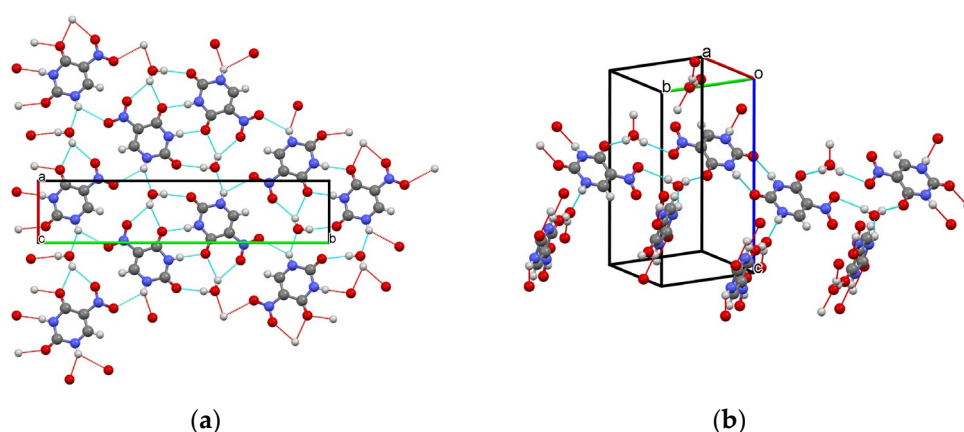


Figure 6. Hydrogen bond network in **(IV)** and **(V)** (a) H-bonded layers in **(IV)**; (b) hydrogen bond network in **(V)**.

Okoth et al. [47,50] have reported the dehydration mechanism and the relative thermal stabilities of the hydrated/anhydro forms of 5NU. They have found that **(IV)** dehydrates to form **(II)**, which then undergoes a phase transformation into **(I)** at ~ 270 °C, prior to decomposition.

4.1.3. 5NU Solvates

This section describes the crystal structure of 5NU solvates (pure hydrates are described in the previous section). All solvent molecules (except dioxane) H-bond to 5NU molecules creating diverse forms of molecular arrangements. Table 3 summarizes the main crystallographic features.

The crystallization of 5NU in aqueous ethanol resulted in a centrosymmetric crystal structure that incorporates both water and ethanol solvate molecules. The crystal structure display two types of molecular assembling via H-bons: a cluster (0D) containing a dimer of 5NU two water molecules and two ethanol molecules, with a M2 motif ($R^2_2(8)$ in graph set analysis), an element that is also seen in compound **(IV)** and 5NU/ethanol chains (1D) in which the nitouracil molecules are not related by an inversion center (Figure 7a,b). The inversion center relates to two distinct chains, therefore annihilating the large dipole that each chain contains.

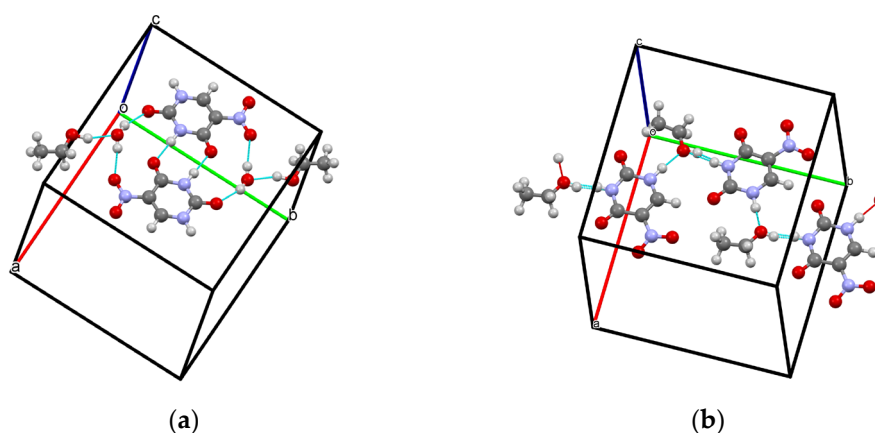


Figure 7. Hydrogen bond network in **(VI)** (a) Dimeric clusters; (b) ethanol/5NU chains.

In the dimethylsulfoxide solvate **(VII)** of 5NU [43,51], the chromophore molecules are assembled in chains via H-bonds in which the oxygen atom of the solvent moiety acts as a bifurcated acceptor (Figure 8). Within the chains the dipole moment does not cancel

but it cancels out in the unit cell (and overall crystal) by the presence of a center of inversion.

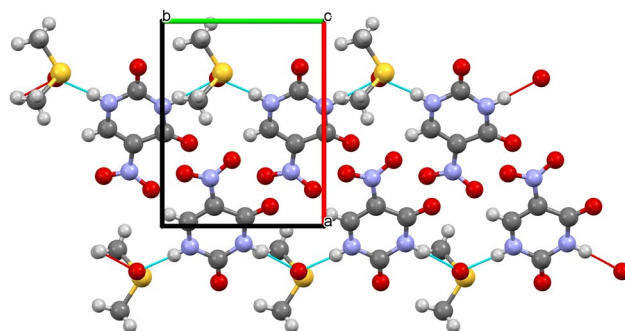


Figure 8. Hydrogen bonded chains in (VII).

In the formamide solvate (VIII) of 5NU, there are six independent molecules (two nitrouracil and four formamide molecules) that interconnect via H-bonds into layers. Figure 9 shows one of such layers with a different color for each symmetry independent residue. As one can see, 5NU molecules do not bond directly; it is the great ability of formamide (with both donors and acceptors) that interconnect all molecules in layers, forming ring patterns. Within the layer, the molecular dipoles cancel out.

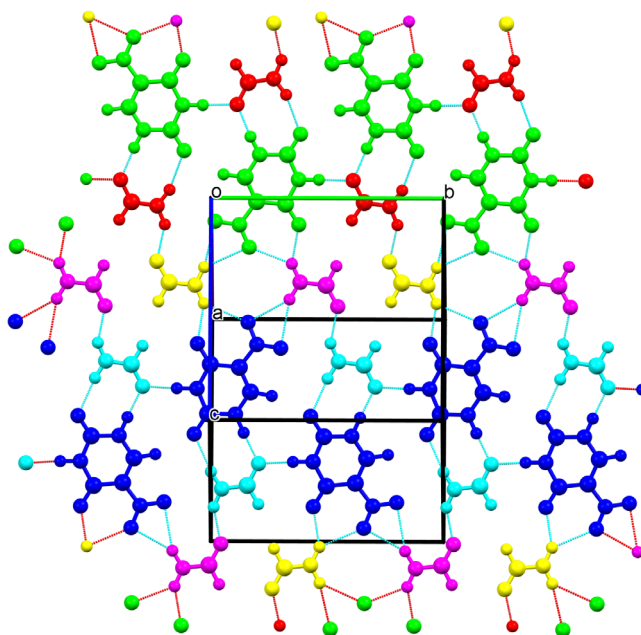


Figure 9. Hydrogen bonded layers in (VIII) with the different colors portraying different residues.

In the pyrimidine solvate (IX) of 5NU (Figure 10), the chromophores assemble in chains forming the M7 motif. In this arrangement, the molecular dipoles do not cancel within the chain but wipe out in the unit cell due to a center of symmetry that relates similar chains. The quantitative descriptors for the patterns containing only one type of hydrogen bond (first or primary level hydrogen-bonding) are $C(6)$, $C(6)$ and $D(2)$.

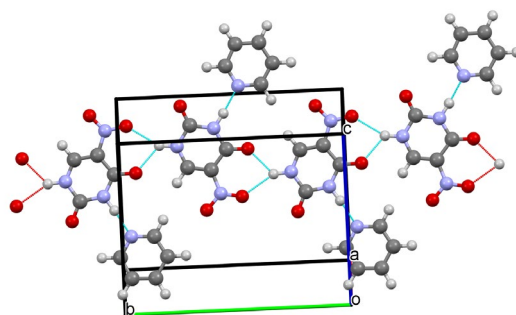


Figure 10. Hydrogen bonded chains in (IX).

In the hemikis(dioxane) solvate (X) of 5NU (Figure 11), the nitrouracil molecules are joined in centrosymmetric dimers with the M3 motif. The dimers are further interconnected in non-planar layers through N-H...O intermolecular bonds. The quantitative descriptors for the first level hydrogen-bonding are $R^2_2(8)$ and $C(4)$. The dioxane solvent molecules are not strongly bonded occupying the center and corners of the unit cell (colored in dark blue in Figure 11a).

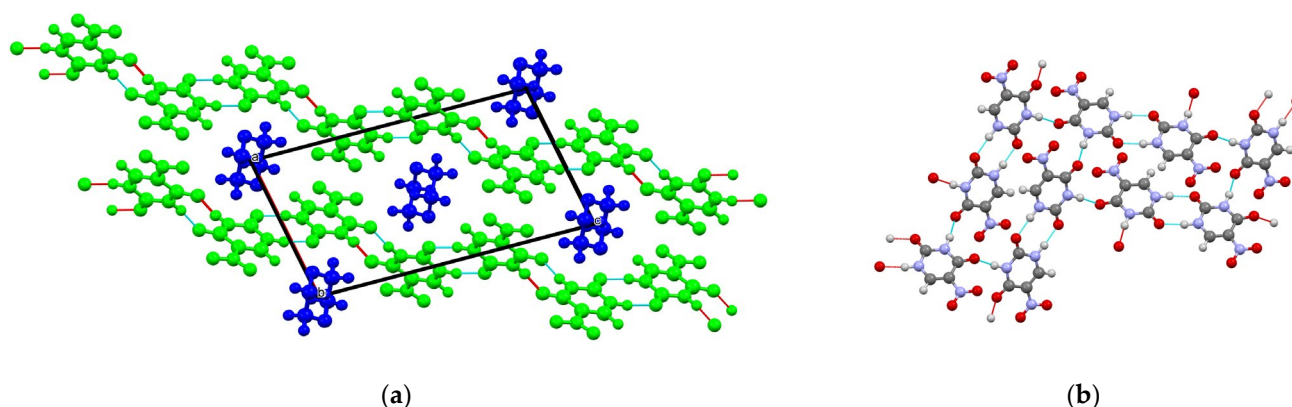


Figure 11. (a) Projection, along *b*, of the crystal packing in (X). (b) Detail of the 5NU H-bonded layer in (X).

4.1.4. 5NU Co-Crystals

We are differentiating cocrystals and solvates based on their physical state of the components. In this section, at least two components are solid at room temperature and a solvent (like water, methanol) has to be added to provide a crystallization medium. Table 4 summarizes the main crystallographic features.

Table 4. Crystallographic data of 5NU solvates.

| Compound/ CCDC Code | Unit Cell (Å, °, Å ³) | Space Group | Dihedral Angle between NO ₂ and Ring (°) | H-Bond Motif | Reference |
|--|--|------------------------------------|---|----------------------------------|-----------|
| 5-Nitrouracil ethanol hemihydrate (VI) JESNAX | a = 11.8264(8) b = 11.8738(8) c = 12.6511(8) β = 98.6960(10) V = 1756.1(2) | <i>P</i> 2 ₁ / <i>c</i> | 4.6(5) 12.3(6) | Clusters with M2 motif Chains | [51] |
| 5-Nitrouracil dimethyl sulfoxide solvate (VIIa) | a = 8.858(1) b = 6.9619(6) c = 15.822(1) | <i>P</i> 2 ₁ / <i>n</i> | 15.80(16) | Chains | [43] |

| | | | | | |
|--|--|----------|------------------|----------------------|------|
| NIMGAR | $\beta = 95.823(8)$ $V = 970.7(1)$ | | | | |
| 5-Nitrouracil dimethyl sulfoxide solvate (VIIb) NIMGAR01 | $a = 8.8723(6)$ $b = 6.9700(5)$ $c = 15.8489(11)$ $\beta = 95.8760(10)$ $V = 974.95(12)$ | $P2_1/n$ | 15.7(2) | Chains | [51] |
| 5-Nitrouracil bis(formamide) (VIII) JESMUQ | $a = 14.1865(8)$ $b = 11.5840(7)$ $c = 12.7907(7)$ $\beta = 94.7750(10)$ $V = 2094.7(2)$ | $P2_1/c$ | 9.0(2) 1.6(2) | Layers | [51] |
| 5-Nitrouracil pyridine (IX) JESMOK | $b = 12.7817(8)$ $c = 10.8938(7)$ $\beta = 97.78$ $V = 1037.08(11)$ | $P2_1/c$ | 5.5(3) | Chains with M7 motif | [51] |
| 5-Nitrouracil hemikis (dioxane) (X) JESMAW | $a = 8.3535(12)$ $b = 6.4277(10)$ $c = 15.703(2)$ $\beta = 101.810(3)$ $V = 825.3(2)$ | $P2_1/n$ | 2.7(6) | Layers with M3 motif | [51] |

In compound **(XI)**, 5-nitrouracil and 5-fluorocytosine molecules are hydrogen bonded in zig-zag chains that run approximately parallel to the ab plane, Table 5. These chains are interconnected via O—H \cdots O interactions to water molecules. The two independent water molecules assemble in a such a way that they form ladders along the c axis (see Figure 12, first level graph descriptors C(2)).

Table 5. Crystallographic data of 5NU co-crystals.

| Compound/ CCDC Code | Unit Cell (\AA , $^\circ$, \AA^3) | Space Group | Dihedral Angle between NO ₂ and Ring ($^\circ$) | H-Bond Motif | Reference |
|---|---|----------------|--|----------------------|-----------|
| 5-Nitrouracil 5-Fluorocytosine dihy- drate (XI) GATMUL | $a = 10.2066(6)$ $b = 28.2758(11)$ $c = 4.7187(3)$ $\beta = 111.293(6)$ $V = 1268.85(12)$ | Cc | 3.8(9) | Chains | [52] |
| 5-Nitrouracil piperazine (XII) JESMEA | $a = 4.3579(5)$ $b = 9.8014(12)$ $c = 12.731(2)$ $\alpha = 94.712(2)$ $\beta = 99.452(2)$ $\gamma = 97.603(2)$ $V = 528.68(11)$ | $P-1$ | 6.4(4) | Chains with M2 motif | [51] |
| 5-Nitrouracil dimethylpiperazine (XIII) JESMIE | $a = 7.1052(14)$ $b = 7.601(2)$ $c = 10.150(2)$ $\alpha = 93.023(3)$ $\beta = 99.452(2)$ $\gamma = 117.689(2)$ | $P-1$ | 18.7(13) | Chains with M1 motif | [51] |

| | | | | | |
|--|---|----------|------------------|-------------------------------------|------|
| 5-Nitrouracil diaza [2.2.2]bicyclooctane (XIV) JESNIF | V = 453.8(2) a = 9.23230(10) b = 9.65980(10) c = 32.2899(6) β = 90.8010(10) V = 2879.40(7) | $P2_1/c$ | 3.0(4) 3.0(4) | 3D network with M2 motif | [51] |
| Aminopyridine 5-Nitrouracil (XV) JESNEB ¹ | a = 9.7466(2) b = 32.0076(6) c = 10.5372(2) β = 122.2060(10) V = 2781.46(10) | $P2_1/c$ | 2.0(7) | Ribbons with M2 ²⁻ motif | [51] |

¹ The deposited crystallographic data contain one extra hydrogen atom.

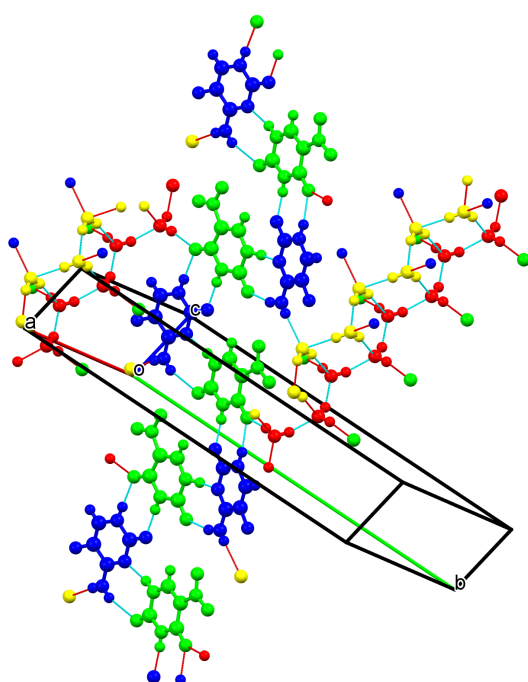


Figure 12. Hydrogen bonded chains in (XI) and ladder formation by water molecules. Different colors portray different residues.

In compound (XII), two independent half-piperazine moieties co-exist in the crystal structure. The piperazine molecules that occupy the unit cell corners (see Figure 13) are connected to 5-nitrouracil via a N-H...N bonds joining 5-nitrouracil dimers (M2 motif, $R_2^2(8)$) in chains. The second piperazine molecule occupy the cell edges without significant interactions.

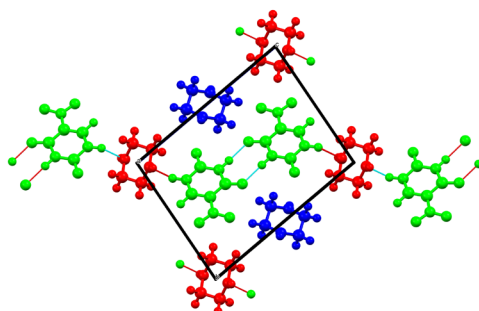


Figure 13. Hydrogen bonded chains in (XII) with different colors portraying different residues.

In the co-crystal of 5-nitrouracil and dimethylpiperazine, the dipole moments of 5NU are again antiparallel aligned in dimers with the M1 motif ($R^2_2(8)$). The dimers are further joined in chains, via H-bonds with the co-former (Figure 14). In 5NU the nitro group is able to rotate around the C–N bond. In this crystal structure, such angle rises up to 18.7(13).

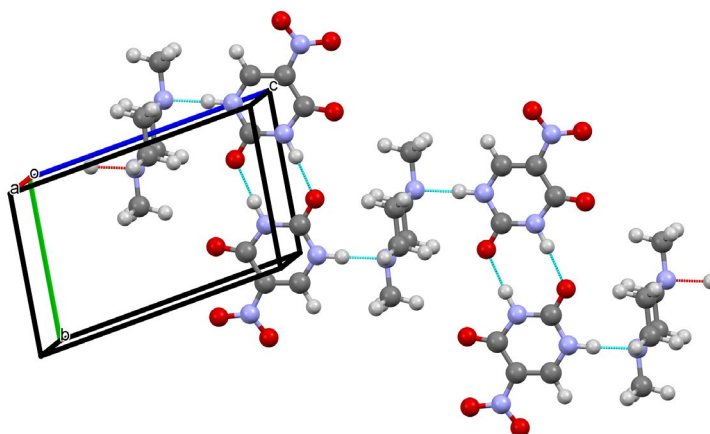


Figure 14. Detail of the 5NU H-bonded chain in (XIII), showing dimers with the M1 motif.

In the co-crystal of 5-nitrouracil and diazabicyclo [2.2.2]octane (DIABCO), there are two symmetry independent 5NU, two symmetry independent DIABCO and four symmetry independent water molecules, all strongly linked via H-bonds. The two independent 5NU are joined in dimers with an almost centrosymmetric M2 motif. The water molecules exhibit an extended network that link all the molecules together. A detail of the H-bond network can be seen in Figure 15b, where only water molecules are visible showing the square grid that they shape.

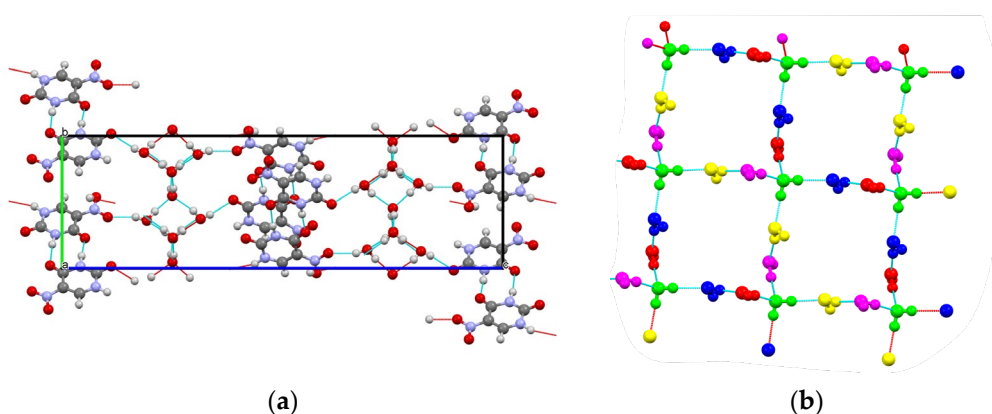


Figure 15. (a) Crystal packing in (XIV), showing dimers with the M2 motif, DIABCO molecules were omitted for clarity. (b) Detail of water molecules framework.

In the co-crystal of 5-nitrouracil and 3-aminopyridine, the coformers are joined in clusters of four neutral molecules that include a dimer of 5-nitrouracil with the M2 motif ($R^2_2(8)$). The cluster are H-bonded to equivalent clusters in a nearly perpendicular orientation forming ribbons (Figure 16).

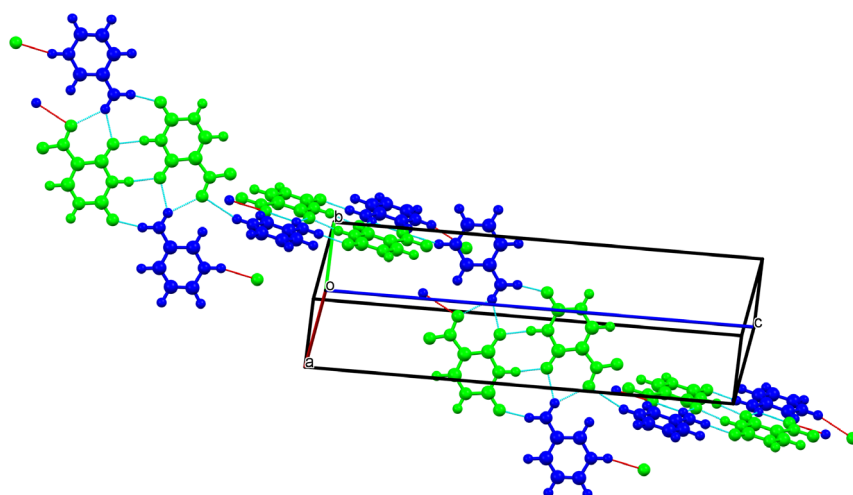


Figure 16. Crystal packing in (XV), showing dimers with the M2 motif.

4.2. 5NU Salts

In this section, we will review the crystal structure and optical properties of 5NU salts, that is, the multicomponent crystals that include at least one ion of 5NU, Table 6. Of the two sites available for ionization in the heterocyclic ring of the 5-nitouracil molecule (N1 and N3, check Figure 1), deprotonation occurs at the more acidic N1 [53]. Although attempts have been made to doubly deprotonate 5-nitouracil, that form has not yet been observed in the solid state. The deprotonation of 5NU has a dramatic effect on the ground state dipolar moment; its magnitude decreases abruptly to less than 0.1 *D* [54].

Table 6. Crystallographic data of L-Histidinium 5-Nitrouacilate salts.

| Compound/ CCDC Code | Unit Cell (Å, °, Å ³) | Space Group | Dihedral Angle between NO ₂ and Ring (°) | H-Bond Motif | Reference |
|--|---|-------------------------|---|--------------------------------|-----------|
| L-Histidinium 5-Nitrouacilate (XVIa) BAQQIW | a = 6.1911(16) b = 7.332(2) c = 13.729(4) β = 99.990(13) V = 613.8(3) At 200K: | <i>P</i> 2 ₁ | 3.33(17) | 3D network | [54] |
| L-Histidinium 5-Nitrouacilate (XVIb) JIMJOH | a = 6.1965(2) b = 7.2965(3) c = 13.7236(5) β = 99.919(2) V = 611.21(4) | <i>P</i> 2 ₁ | 3.38(11) | 3D network | [55] |
| L-Histidinium 5-Nitrouacilate (XVII) BAQQIW01 | a = 5.1555(9) b = 8.3627(15) c = 14.323(3) α = 83.206(5) β = 89.993(5) γ = 88.549(5) V = 612.99(19) | <i>P</i> 1 | 2.02(2) 3.9(2) | 3D network with M1 motif | [55] |

4.2.1. L-Histidinium 5-Nitrouracilate

In 2011, we have deliberately tried a co-crystallization of 5NU with L-histidine (a chiral amino acid) to force the crystal packing in a non-centrosymmetric environment [54]. Adding both reagents in a 1:1 proportion in an aqueous solution yielded pink crystals. The crystal structure determination revealed that L-histidine acquires a positive charge by the transfer of one hydrogen atom from the 5NU moiety that turns negative. L-histidine, in the zwitterionic form of L-histidinium cation assembles along the 2_1 axis via H-bonds between the amino group and the carboxylate group of neighboring cations. The anions are encapsulated within the cationic layers hampering direct interaction between the charged 5NU (Figure 17). Nonetheless, the almost co-planarity of imidazolium and the pyrimidine rings (at a close distance of 3.5 Å) will have a significant effect on the charge distribution of the ionic pair in an excited state. Thus, the NLO enhanced properties of the crystal are interpreted (as well as a large vibrational circular dichroism response) as a play of two energetic levels, the ground state and a low-lying first excited state where charge migrates from one ring to the adjacent one (Figure 18).

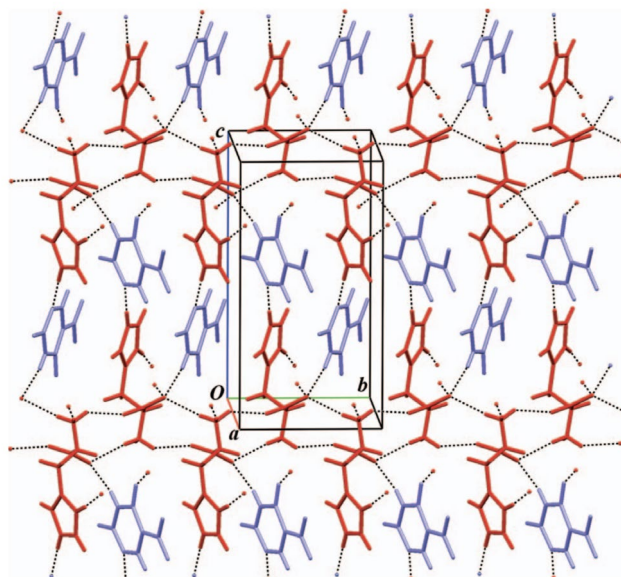


Figure 17. Guest-host structure of L-His+5NU⁻ (XVIa). The anions (blue) are encapsulated between the cationic layers (red) in a polar herringbone motif along the b axis. Reprinted with permission from Ref. [54], 2012, AIP publishing.

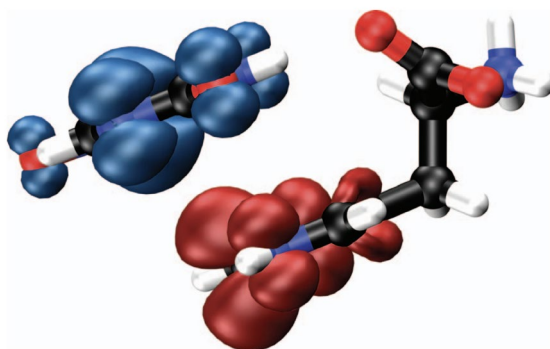


Figure 18. Difference density plot (isovalue 0.004) between ground and excited state (S1-S0) of L-His+5NU⁻ obtained from a TD-DFT (X3LYP/6-311++G**) calculation. Blue indicates positive values and red negative values. Reprinted with permission from Ref. [54], 2012, AIP publishing.

The crystal structure of (XVII) contains two independent formula units [55]. The two symmetry independent 5-nitrouracil anions form pseudo-symmetric dimers linked with double N–H···O type hydrogen bonds, with a $M1^{2-}$ motif (Figure 19). At the primary level, graph patterns corresponded to chains described with $C(5)$ and $C(7)$.

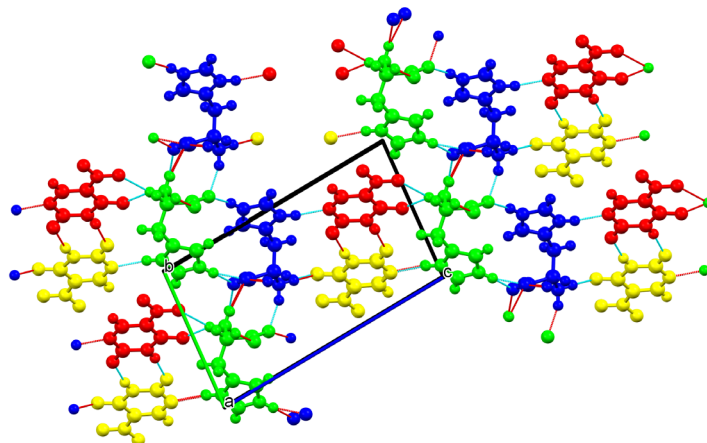


Figure 19. Detail of the 3D H-bond network showing dimer formation in (XVII).

4.2.2. 5NU Salts of Guanidine Derivatives

Guanidinium 5-Nitrouracilate Monohydrate

The crystal structure of the compound guanidinium 5-nitrouracilate monohydrate (XVIII), (Table 7, Figure 20), belongs to the triclinic system with the centrosymmetric space group $P\bar{1}$. The asymmetric unit consists of one guanidinium cation with a 5-nitrouracilate counter-ion and a water molecule.

Table 7. Crystal data and structure refinement parameters for (XVIII) and (XIV).

| Compound | Guanidinium 5-Nitrouracilate Monohy- drate (XVIII) | Phenylguanidinium 5-Nitrouracilate Monohydrate (XIX) |
|--|---|--|
| Temperature/K | 293 | 293 |
| Empirical formula | $C_5H_{10}N_6O_5$ | $C_{11}H_{14}N_6O_5$ |
| Formula weight | 234.19 | 310.28 |
| Wavelength/Å | 0.71073 | 0.71073 |
| Crystal system | Triclinic | Monoclinic |
| Space group | $P\bar{1}$ | $P2_1/c$ |
| a/Å | 3.65270(10) | 9.7466(2) |
| b/Å | 11.1035(3) | 32.0076(6) |
| c/Å | 11.8152(3) | 10.5372(2) |
| a/° | 82.383(2) | 90 |
| b/° | 86.406(2) | 122.2060(10) |
| c/° | 89.405(2) | 90 |
| Volume/Å ³ | 474.03(2) | 2781.46(10) |
| Z | 2 | 8 |
| Calculated density/(g/cm ³) | 1.641 | 1.404 |
| Absorption coeffi- cient/mm ⁻¹ | 0.145 | 0.105 |
| F(000) | 244 | 1374 |

| | | |
|--|--|---|
| θ range for data collection/deg. | 1.74–27.46 | 2.37–28.74 |
| Index ranges | $-4 < h < 4, -14 < k < 14, -15 < l < -12 < h < 13, -43 < k < 43, -15 < l < 15$ | |
| Reflections collected/unique | 9678/1545 | 89166/4531 |
| Completeness to θ_{\max} | 100% | 99.5% |
| Data/restraints/parameters | 1545/0/173 [$R(\text{int}) = 0.0357$] | 4531/0/454 [$R(\text{int}) = 0.0311$] |
| Goodness-of-fit on F^2 | 1.050 | 1.0026 |
| Final R index [$I > 2\sigma(I)$] | $R1 = 0.0363$ $wR2 = 0.0890$ | $R1 = 0.0441$ $wR2 = 0.1172$ |
| R index (all data) | $R1 = 0.0591$ $wR2 = 0.1003$ | $R1 = 0.0786$ $wR2 = 0.1378$ |
| Largest diff. peak and hole ($e \text{ \AA}^{-3}$) | -0.162 and 0.256 | -0.198 and 0.215 |

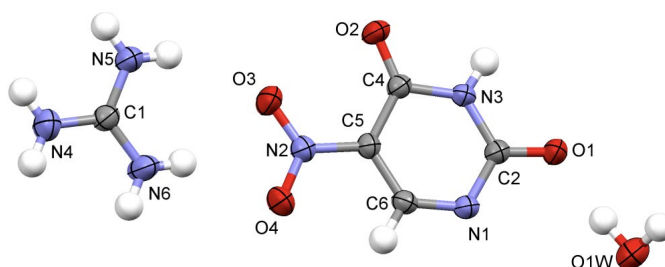


Figure 20. Asymmetric unit of guanidinium 5-nitrouracilate monohydrate (XVIII). Displacement ellipsoids are drawn at the 50% probability level.

There are two sites available for deprotonation in the heterocyclic ring of the 5-nitrouracil molecule (N1 and N3) and it occurs at the more acidic N1. In the anion the pyrimidine ring is almost planar and the nitro group is rotated $2.8(2)^\circ$ out of the plane of the uracil fragment. The ions and the water molecules are linked by $\text{N}-\text{H}\cdots\text{O}$ and $\text{N}-\text{H}\cdots\text{N}$ hydrogen bonds forming layers approximately parallel to the plane (112), see Figure 21a,b, Table 8. These layers are linked via the water molecules. All six potential donor sites of the guanidinium cation participate in hydrogen bonds. In this structure, the full hydrogen bonding capability of the 5-nitrouracilate anion is also used. Each cation is hydrogen-bonded to three anions and one water molecule. The anions are linked in pairs across an inversion center forming rings of descriptor $R^2_2(8)$, and also to three cations and two water molecules.

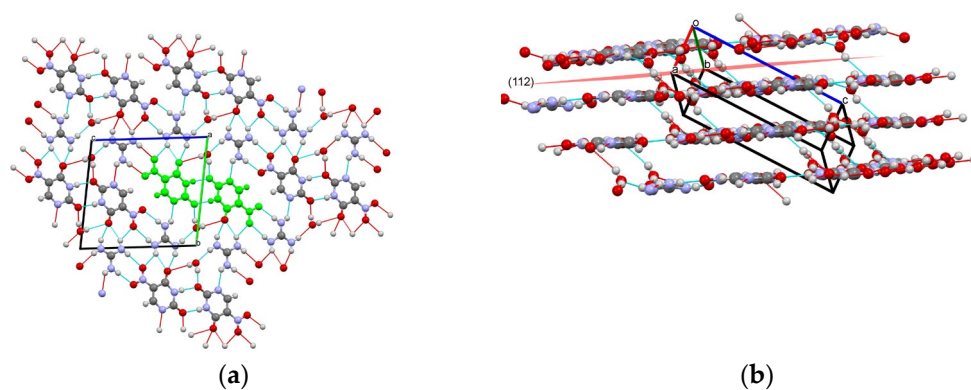


Figure 21. (a) A packing diagram for guanidinium 5-nitrouracilate monohydrate, viewed down the a axis, showing the layer formation. Hydrogen bonds are shown as dashed lines. One of the centrosymmetric dimers is highlighted in solid green. (b) Layers seen from one of the sides.

Table 8. Hydrogen bond geometry of guanidinium 5-nitrouracilate monohydrate (Å, °).

| D–H···A | D–H | H···A | D···A | D–H···A |
|----------------------------|-----------|-----------|------------|-----------|
| N3–H3···O1 ⁱ | 0.857(17) | 1.984(18) | 2.8387(15) | 174.4(15) |
| N4–H4B···O1W ⁱⁱ | 0.89(2) | 2.01(2) | 2.884(2) | 167.3(18) |
| N4–H4A···O2 ⁱⁱⁱ | 0.87(2) | 2.26(2) | 3.004(2) | 143.9(17) |
| N5–H5A···N1 ⁱⁱ | 0.86(2) | 2.35(2) | 3.0626(18) | 140.4(17) |
| N5–H5B···O4 ^{iv} | 0.89(2) | 2.07(2) | 2.9590(19) | 175.0(18) |
| N6–H6A···O2 ⁱⁱⁱ | 0.924(19) | 2.132(19) | 2.9773(18) | 151.5(16) |
| N6–H6A···O3 ⁱⁱⁱ | 0.924(19) | 2.274(18) | 2.9655(17) | 131.2(15) |
| N6–H6B···O3 ^{iv} | 0.86(2) | 2.30(2) | 3.1445(18) | 171.6(17) |
| O1W–H1W···O1 | 0.86(3) | 1.90(3) | 2.7522(17) | 171(2) |
| O1W–H2W···O2 ^v | 0.82(2) | 2.44(3) | 3.2104(18) | 157(2) |

Symmetry codes *i*: 2 – *x*, 1 – *y*, –*z*; *ii*: 1 – *x*, 1 – *y*, 1 – *z*; *iii*: 2 – *x*, –*y*, 1 – *z*; *iv*: 1 + *x*, *y*, *z*; *v*: 1 – *x*, 1 – *y*, –*z*.

Phenylguanidinium 5-Nitrouracilate Monohydrate

The crystals of phenylguanidinium 5-nitrouracilate monohydrate (**XIX**) are monoclinic with the space group $P2_1/c$. The asymmetric unit cell has two phenylguanidinium cations, two 5-nitrouracilate anions and two water molecules (Table 7, Figure 22). The two symmetry-independent phenylguanidinium cations have very different conformations as evidenced by the values of the torsion angle C7–N8–C8–C13: 61.4(2)° for cation C and –51.0(2)° for D.

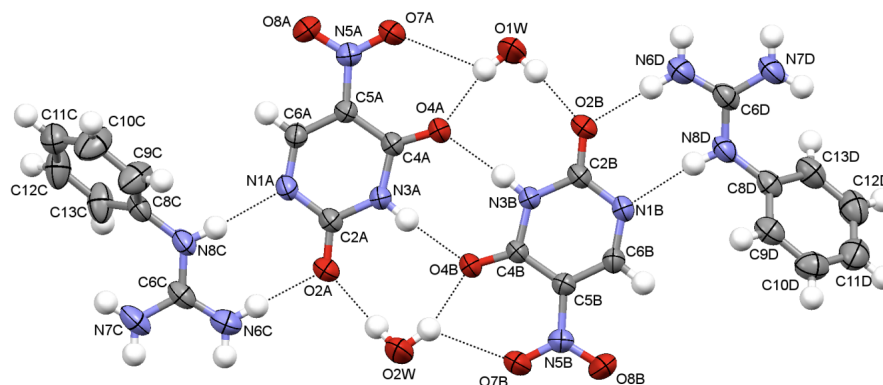


Figure 22. A plot with the symmetry-independent molecular units of phenylguanidinium 5-nitrouracilate monohydrate. Displacement ellipsoids are drawn at the 50% probability level. Hydrogen bonds are shown as dashed lines.

In both symmetry-independent anions, the pyrimidine ring is almost planar and the nitro group is rotated out of the plane of the uracil fragment 1.3(1)° and 6.7(1)° for anions A and B, respectively. There is an extensive network of N–H···O and N–H···N hydrogen bonds linking the ions and the water molecules into ribbons (Figure 23, Table 9). The anions are linked in pairs forming rings of descriptor $R^2_2(8)$, with the $M2^{2-}$ motif.

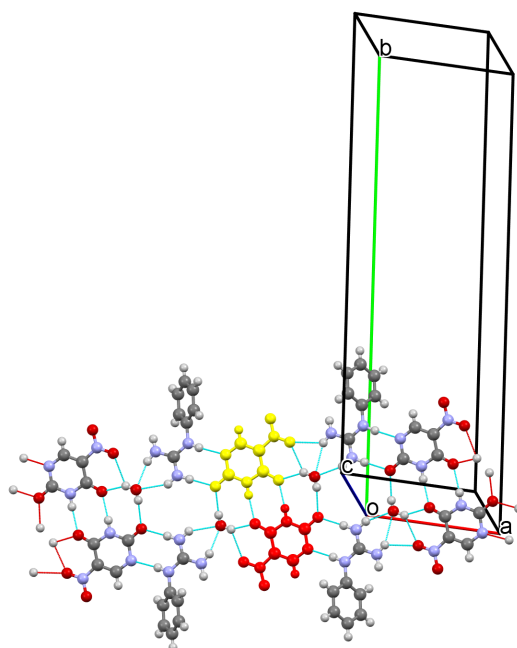


Figure 23. A detail of the hydrogen bonded ribbons in (XIX). 5NU dimer is highlighted in solid colors (yellow and red).

Table 9. Hydrogen bond geometry of phenylguanidinium 5-nitrouracilate monohydrate ($\text{\AA},^\circ$).

| D—H...A | D—H | H...A | D...A | D—H...A |
|-------------------------------|-----------|-----------|------------|-----------|
| O1W—H1...O4A | 0.82(4) | 1.99(4) | 2.7274(17) | 150(3) |
| O1W—H1A...O7A | 0.82(4) | 2.42(3) | 3.0398(19) | 133(3) |
| O1W—H1B...O2B ⁱ | 0.75(3) | 2.10(3) | 2.8450(19) | 170(4) |
| O2—H2A...O4B | 0.87(3) | 2.03(3) | 2.7876(17) | 146(3) |
| O2W—H2A...O7B | 0.87(3) | 2.29(3) | 2.9731(18) | 136(3) |
| O2W—H2B...O2A ⁱ | 0.74(3) | 2.15(3) | 2.8746(18) | 167(3) |
| N3—H3...O4B ⁱ | 0.893(17) | 1.961(18) | 2.8508(15) | 174.0(15) |
| N3B—H3B...O4A ⁱ | 0.870(17) | 1.993(17) | 2.8606(15) | 174.1(15) |
| N6C—H6C1...O2W ⁱⁱ | 0.88(2) | 2.09(2) | 2.930(2) | 159.1(18) |
| N6C—H6C2...O2A | 0.93(2) | 1.91(2) | 2.8354(19) | 176.8(18) |
| N7C—H7C...O7B ⁱⁱ | 0.85(2) | 2.39(2) | 3.0006(18) | 129.4(18) |
| N7C—H7C1...O2W ⁱⁱ | 0.85(2) | 2.34(2) | 3.118(3) | 153(2) |
| N8—H8C...N1A | 0.905(19) | 2.015(19) | 2.9138(17) | 172.0(16) |
| N6D—H6D1...O1W ⁱⁱⁱ | 0.86(2) | 2.27(2) | 3.020(2) | 145.9(17) |
| N6D—H6D2...O2B ^{iv} | 0.89(2) | 1.92(2) | 2.8082(18) | 177.0(19) |
| N7D—H7D1...O1W ⁱⁱⁱ | 0.86(2) | 2.04(2) | 2.871(2) | 162(2) |
| N7D—H7D1...O7A ⁱⁱⁱ | 0.86(2) | 2.55(2) | 3.0295(17) | 116.4(16) |
| N8D—H8D...N1B ^{iv} | 0.873(19) | 2.080(19) | 2.9495(17) | 173.9(17) |

Symmetry codes *i*: $-x + 1, -y, -z + 1$; *ii*: $x - 1, y, z$; *iii*: $x - 1, y, z - 1$; *iv*: $x + 1, y, z + 1$.

Diphenylguanidinium 5-Nitrouracilate Dihydrate

The crystals of diphenylguanidinium 5-nitrouracilate [56] incorporate two water molecules per asymmetric unit cell, aggregating anions and cations into H-bonded slabs that stack along the *c* axis (Table 10, Figure 24). 5NU ions are strongly H-bonded into dimers, showing the M1²⁻ (*R*²₂(8)) motif.

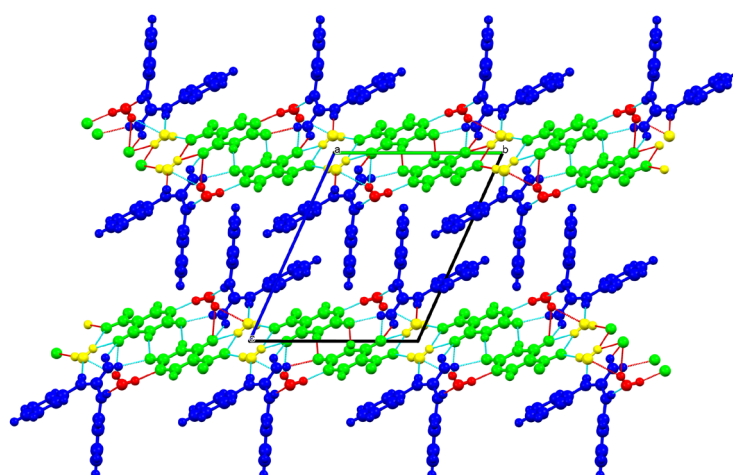


Figure 24. Crystal packing of (XX) viewed along the a axis. 5NU ions are shown in solid green, highlighting the dimer formation.

Table 10. Crystallographic data of 5NU salts of guanidine derivatives.

| Compound/ CCDC Code | Unit Cell (\AA , $^\circ$, \AA^3) | Space Group | Dihedral Angle between NO_2 and Ring ($^\circ$) | H-Bond Motif | Reference |
|---|---|----------------|--|---|-----------|
| Guanidinium 5-Nitrouracilate monohydrate (XVIII) CCDC 2222685 | $a = 3.65270(10)$ $b = 11.1035(3)$ $c = 11.8152(3)$ $\alpha = 82.383(2)$ $\beta = 86.406(2)$ $\gamma = 89.405(2)$ $V = 474.03(2)$ | $P-1$ | 2.8(2) | 3D network with M1^{2-} motif | This work |
| Phneylguanidinium 5-Nitrouracilate monohydrate (XIX) CCDC 2222686 | $a = 9.7466(2)$ $b = 32.0076(6)$ $c = 10.5372(2)$ $\beta = 122.2060(10)$ $V = 2781.46(10)$ | $P2_1/c$ | 1.3(1) 6.7(1) | Ribbons with M2^{2-} motif | This work |
| Diphenylguanidinium 5-Nitrouracilate dihydrate (XX) BAQPAN | $a = 6.6889(2)$ $b = 11.5839(3)$ $c = 13.7723(3)$ $\alpha = 112.910(2)$ $\beta = 91.715(2)$ $\gamma = 104.582(2)$ $V = 941.44(4)$ | $P-1$ | 6.04(19) | Slabs with M1^{2-} motif. | [56] |
| Triphenylguanidinium 5-Nitrouracilate (XXI) WIZXAF | $a = 10.7495(4)$ $b = 15.6892(7)$ $c = 15.5624(7)$ $\beta = 123.456(3)$ $V = 2189.74(18)$ | $P2_1/c$ | 11.4(2) | Columns | [57] |

Triphenylguanidinium 5-Nitrouracilate

The anions and cations are linked into columns running parallel to the b axis, via hydrogen bonds involving all the NH groups of the guanidinium fragment, the carbonyl O atoms and the deprotonated N atom of the anion [57]. The 5NU ions are lined up within

each column without direct interionic interactions (Figure 25). A center of symmetry relates the columns in the crystal, obliterating the overall dipole moment.

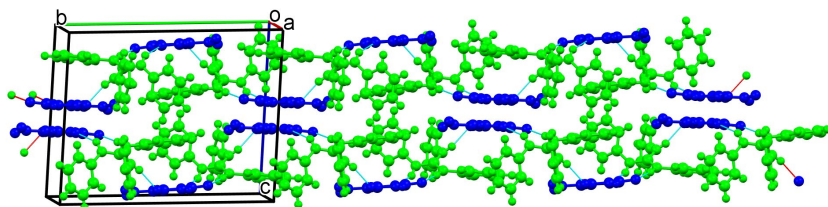


Figure 25. Columnar formation of (XXI) viewed along the *a* axis. 5NU ions are shown in solid blue, triphenylguanidinium ions are depicted in solid green.

4.2.3. Other 5NU Salts

Cytosinium 5-Nitrouracilate

The crystals that grow from a 1:1 aqueous solution of cytosine and 5-nitrouracil [52] after heating, stirring and refluxing, belong to a subclass that intersects the family of co-crystals, salts and solvates [58]. The asymmetric unit of (XXII) contains one neutral molecule of cytosine, one charged ion of cytosine, one neutral molecule of 5-nitrouracil, one charged ion of 5-nitrouracil and two water molecules, see Table 11 for more parameters. In Figure 26, one can see how these molecules assemble in the solid: they are all hydrogen bonded in layers parallel to the *bc* plane. The neutral/charged ion of the same species are strongly bonded together by sharing a hydrogen atom between the protonated/deprotonated sites (yellow/red for cytosine and blue/green for nitrouracil for protonated/deprotonated forms in Figure 26).

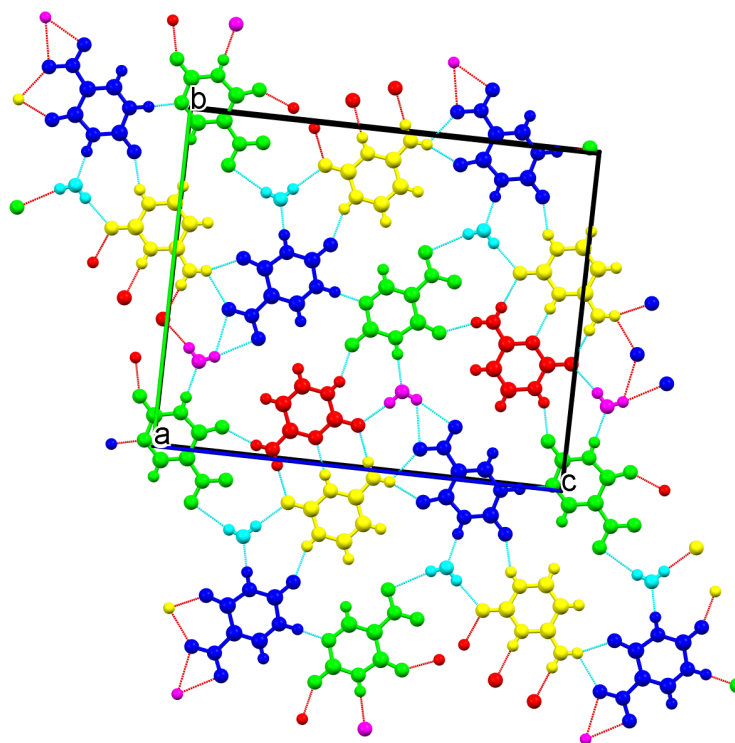


Figure 26. Detail of one of the layers of (XXI) viewed along the *a* axis. Different colors were used for non-equivalent residues.

In order to probe if a charge distribution occur in the neutral/charged pair, we have performed ab-initio calculations using as input the atomic coordinates retrieved from X-ray determination (see Section 3.3 for technical details). The results show a moment of circa 5 D very similar to the neutral molecule alone.

Table 11. Crystallographic data of more 5NU salts.

| Compound/ CCDC Code | Unit Cell (Å, °, Å ³) | Space Group | Dihedral Angle between NO ₂ and Ring (°) | H-Bond Motif | Reference |
|--|--|----------------|---|---|-----------|
| Cytosinium 5-Nitrouracilate Cytosine 5-Nitrouracil dihydrate (XXII) GATMOF | a = 3.65270(10) b = 11.1035(3) c = 11.8152(3) α = 82.383(2) β = 86.406(2) γ = 89.405(2) V = 474.03(2) | P-1 | 1.2(5) 1.8(5) | Layers (with neu- tral/charged pairs) | [52] |
| Benzamidinium 5-Nitrouracilate dihydrate (XXIII) TUWDEV | a = 4.3625(4) b = 10.4461(11) c = 13.8556(12) α = 78.551(7) β = 86.841(8) γ = 84.051(7) V = 615.13(10) | P-1 | 1.6(3) | Ribbons with M2 ²⁻ motif. | [59] |

Benzamidinium 5-Nitrouracilate

The benzamidinium and 5-nitrouracilate ions aggregate in ribbons profusely H-bonded (Figure 27). One can spot the dimer formation with the M2²⁻ motif ($R^2_2(8)$) [59]. Ions within the dimers are related by an inversion center.

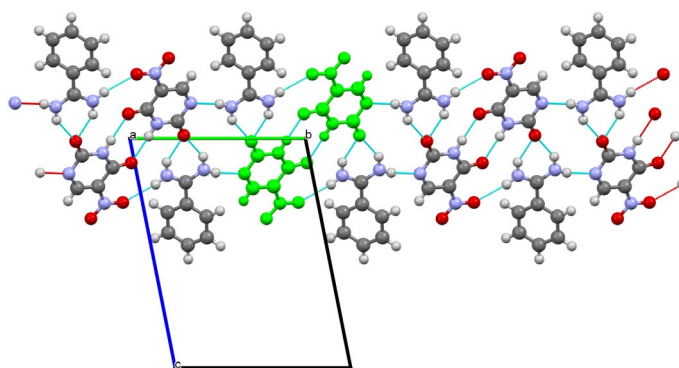


Figure 27. Detail of one of the ribbons of (XXIII) viewed along the *a* axis. One of the 5-nitrouracilate dimers is highlighted in solid green.

5. Conclusions

5-nitrouracil is an achiral molecule with large optical response and its properties could be translated to a solid, ensuring that it remains neutral in a chiral environment. Such an environment not only enhances the ground dipolar moment but also assures that a nonzero second-harmonic generation can be obtained. From an overview of all reported structures so far, one can conclude that changing the crystallization solvent has a dramatic influence on the molecular packing, either by promoting an achiral assembling (acetonitrile), or by avoiding the pairing of dipolar moments (sulfoxide, formamide). For 5-

nitrouracil, exploring polymorphism (a pervasive phenomenon) looks like the promising route to discover molecular environments that boost second-order nonlinear optical susceptibilities. Co-crystallization with a neutral molecule has not (yet) shown the ability to induce a chiral environment. Regrettably, upon losing one H⁺ and gaining an overall negative charge, the dipole moment of 5-nitrouracil drops substantially. However, the electron cloud of 5NU⁻ can still be quite affected by an electric field. Salt formation with a chiral zwitterion has shown the phenomenon of through space charge transfer, with the charge moving from one ion to the other in piles of stacked rings with strong *p-p* interactions. This ionic assembling has shown that both linear and nonlinear optical responses are greatly enhanced.

Author Contributions: Conceptualization, M.R.S. and P.P.d.S.; Investigation, M.R.S. and P.P.d.S.; Writing, M.R.S. and P.P.d.S. All authors have read and agreed to the published version of the manuscript.

Funding: This research was funded by FCT through the projects UIDB/04564/2020 and UIDP/04564/2020.

Data Availability Statement: Experimental data is available included in the CIF files.

Conflicts of Interest: The authors declare no conflicts of interest.

References

1. Franken, P.A.; Hill, A.E.; Peters, C.; Weinreich, G. Generation of Optical Harmonics. *Phys. Rev. Lett.* **1961**, *7*, 118.
2. Boyd, R.W. Chapter 1—The Nonlinear Optical Susceptibility. In *Nonlinear Optics*, 4th ed.; Boyd, R.W., Ed.; Academic Press: Cambridge, MA, USA, 2020; pp. 1–64. ISBN 978-0-12-811002-7.
3. Rentzepis, P.M.; Pao, Y.H. Laser-Induced Optical Second Harmonic Generation in Organic Crystals. *Appl. Phys. Lett.* **1964**, *5*, 156–158. <https://doi.org/10.1063/1.1754096>.
4. Shirota, Y.; Kageyama, H. 1—Organic Materials for Optoelectronic Applications: Overview. In *Handbook of Organic Materials for Electronic and Photonic Devices*, 2nd ed.; Ostroverkhova, O., Ed.; Woodhead Publishing: Sawston, UK, 2019; pp. 3–42. ISBN 978-0-08-102284-9.
5. Nicoud, J.F.; Twieg, R.J. Design and Synthesis of Organic Molecular Compounds for Efficient Second-Harmonic Generation. In *Nonlinear Optical Properties of Organic Molecules and Crystals*; Elsevier: Amsterdam, The Netherlands, 1987; pp. 227–296.
6. Liu, Y.; Yuan, Y.; Tian, X.; Yuan, J.; Sun, J. High First-Hyperpolarizabilities of Thiobarbituric Acid Derivative-Based Donor- π -Acceptor Nonlinear Optical-Phores: Multiple Theoretical Investigations of Substituents and Conjugated Bridges Effect. *Int. J. Quantum. Chem.* **2020**, *120*, e26176. <https://doi.org/10.1002/qua.26176>.
7. Bureš, F. Fundamental Aspects of Property Tuning in Push-Pull Molecules. *RSC Adv.* **2014**, *4*, 58826–58851.
8. Karna, S.P.; Prasad, P.N.; Dupuis, M. Nonlinear Optical Properties of P-nitroaniline: An Ab Initio Time-dependent Coupled Perturbed Hartree–Fock Study. *J. Chem. Phys.* **1991**, *94*, 1171–1181. <https://doi.org/10.1063/1.460024>.
9. Woodford, J.N.; Pauley, M.A.; Wang, C.H. Solvent Dependence of the First Molecular Hyperpolarizability of P-Nitroaniline Revisited. *J. Phys. Chem. A* **1997**, *101*, 1989–1992. <https://doi.org/10.1021/jp9639861>.
10. Potter, K.S.; Simmons, J.H. Chapter 8—Nonlinear Optical Processes in Materials. In *Optical Materials*, 2nd ed.; Potter, K.S., Simmons, J.H., Eds.; Elsevier: Amsterdam, The Netherlands, 2021; pp. 429–478, ISBN 978-0-12-818642-8.
11. Baptista, R.M.F.; Bernardo, C.R.; Belsley, M.S.; de Matos Gomes, E. Electrospun Fibers with Highly Polarized Second Harmonic Light from 2-Amino-4-Nitroaniline and 3-Nitroaniline Nanocrystals Embedded in Poly-L-Lactic Acid Polymer. *Opt. Mater.* **2021**, *116*, 111089. <https://doi.org/10.1016/j.optmat.2021.111089>.
12. Dalton, L.; Benight, S. Theory-Guided Design of Organic Electro-Optic Materials and Devices. *Polymers* **2011**, *3*, 1325–1351. <https://doi.org/10.3390/polym3031325>.
13. Verbiest, T.; Houbrechts, S.; Kauranen, M.; Clays, K.; Persoons, A. Second-Order Nonlinear Optical Materials: Recent Advances in Chromophore Design. *J. Mater. Chem.* **1997**, *7*, 2175–2189.
14. Chemla, D.S.; Oudar, J.L.; Jerphagnon, J. Origin of the Second-Order Optical Susceptibilities of Crystalline Substituted Benzene. *Phys. Rev. B* **1975**, *12*, 4534–4546. <https://doi.org/10.1103/PhysRevB.12.4534>.
15. Zyss, J.; Oudar, J.L. Relations between Microscopic and Macroscopic Lowest-Order Optical Nonlinearities of Molecular Crystals with One- or Two-Dimensional Units. *Phys. Rev. A* **1982**, *26*, 2028–2048. <https://doi.org/10.1103/PhysRevA.26.2028>.
16. Champagne, B.; Bishop, D.M. Calculations of Nonlinear Optical Properties for the Solid State. In *Advances in Chemical Physics*; John Wiley & Sons: Hoboken, NJ, USA, 2003; pp. 41–92. ISBN 9780471428015.
17. Kleinman, D.A. Nonlinear Dielectric Polarization in Optical Media. *Phys. Rev.* **1962**, *126*, 1977–1979. <https://doi.org/10.1103/PhysRev.126.1977>.
18. Jerphagnon, J. Optical Second-Harmonic Generation in Isocyclic and Heterocyclic Organic Compounds. *IEEE J. Quantum Electron.* **1971**, *7*, 42–43. <https://doi.org/10.1109/JQE.1971.1076539>.

19. Puccetti, G.; Perigaud, A.; Badan, J.; Ledoux, I.; Zyss, J. 5-Nitrouracil: A Transparent and Efficient Nonlinear Organic Crystal. *J. Opt. Soc. Am. B* **1993**, *10*, 733–744.
20. Cockayne, B. The Growth of Single Crystals by R. A. Laudise. *J. Appl. Crystallogr.* **1972**, *5*, 53. <https://doi.org/10.1107/S0021889872008738>.
21. Arechi, F.T.; Schulz-Dubois, E.O.; Stith, M.L. *Laser Handbook*; North-Holland Publ. Co.: Amsterdam, The Netherlands, 1972; ISBN 0720402131.
22. Zumsteg, F.C.; Bierlein, J.D.; Gier, T.E. KxRb1-xTiOPO4: A New Nonlinear Optical Material. *J. Appl. Phys.* **1976**, *47*, 4980–4985. <https://doi.org/10.1063/1.322459>.
23. Bierlein, J.D.; Vanherzeele, H. Potassium Titanyl Phosphate: Properties and New Applications. *J. Opt. Soc. Am. B* **1989**, *6*, 622–633. <https://doi.org/10.1364/JOSAB.6.000622>.
24. Cassidy, C.; Halbout, J.M.; Donaldson, W.; Tang, C.L. Nonlinear Optical Properties of Urea. *Opt. Commun.* **1979**, *29*, 243–246. [https://doi.org/10.1016/0030-4018\(79\)90027-0](https://doi.org/10.1016/0030-4018(79)90027-0).
25. Catella, G.C.; Bohn, J.H.; Luken, J.R. Tunable High-Power Urea Optical Parametric Oscillator. *IEEE J. Quantum Electron.* **1988**, *24*, 1201–1203. <https://doi.org/10.1109/3.245>.
26. Zyss, J.; Chemla, D.S.; Nicoud, J.F. Demonstration of Efficient Nonlinear Optical Crystals with Vanishing Molecular Dipole Moment: Second-harmonic Generation in 3-methyl-4-nitropyridine-1-oxide. *J. Chem. Phys.* **1981**, *74*, 4800–4811. <https://doi.org/10.1063/1.441759>.
27. Rao, T.S.; Rando, R.F.; Huffman, J.H.; Revankar, G.R. Synergistic Effect of 5-Nitro-2'-Deoxyuridine with Ganciclovir Against Human Cytomegalovirus In Vitro. *Nucleosides Nucleotides* **1995**, *14*, 1997–2008. <https://doi.org/10.1080/15257779508010719>.
28. Smiley, J.A.; Angelot, J.M.; Cannon, R.C.; Marshall, E.M.; Asch, D.K. Radioactivity-Based and Spectrophotometric Assays for Isoorotate Decarboxylase: Identification of the Thymidine Salvage Pathway in Lower Eukaryotes. *Anal. Biochem.* **1999**, *266*, 85–92. <https://doi.org/10.1006/abio.1998.2935>.
29. Šebesta, K.; Bauerová, J.; Šormová, Z. Inhibition of Uracil and Thymine Degradation by Some 5-Substituted Uracil Analogues. *Biochim. Biophys. Acta* **1961**, *50*, 393–394. [https://doi.org/10.1016/0006-3002\(61\)90352-3](https://doi.org/10.1016/0006-3002(61)90352-3).
30. Singh, U.P.; Singh, B.N.; Sastry, M.S.; Ghose, A.K. X-Ray Diffraction Studies on Metal Complexes of 5-Nitrouracil. *Cryst. Res. Technol.* **1995**, *30*, K13–K15. <https://doi.org/10.1002/crat.2170300126>.
31. Kattan, D.; Alcolea Palafox, M.; Rathor, S.K.; Rastogi, V.K. A DFT Analysis of the Molecular Structure, Vibrational Spectra and Other Molecular Properties of 5-Nitrouracil and Comparison with Uracil. *J. Mol. Struct.* **2016**, *1106*, 300–315. <https://doi.org/10.1016/j.molstruc.2015.10.096>.
32. Copik, A.; Suwinski, J.; Walczak, K.; Bronikowska, J.; Czuba, Z.; Król, W. Synthesis of 1-(2-hydroxy-3-methoxypropyl)uracils and Their Activity against H1210 and Macrophage Raw 264.7 Cells. *Nucleosides Nucleotides Nucleic Acids* **2002**, *21*, 377–383. <https://doi.org/10.1081/NCN-120006831>.
33. Murti, Y.; Vijayan, C. From Optics to Photonics. In *Essentials of Nonlinear Optics*; John Wiley & Sons: New Jersey, USA, 2014; pp. 1–9, ISBN 9781118902332.
34. Sheldrick, G.M. *SADABS, Software for Empirical Absorption Corrections*; University of Göttingen, Göttingen, Germany, 1996.
35. Sheldrick, G.M. Crystal Structure Refinement with SHELXL. *Acta Crystallogr. Sect. C* **2015**, *71*, 3–8. <https://doi.org/10.1107/S2053229614024218>.
36. Spek, A.L. Structure Validation in Chemical Crystallography. *Acta Crystallogr. Sect. D* **2009**, *65*, 148–155. <https://doi.org/10.1107/S090744490804362X>.
37. Macrae, C.F.; Edgington, P.R.; McCabe, P.; Pidcock, E.; Shields, G.P.; Taylor, R.; Towler, M.; van de Streek, J. Mercury: Visualization and Analysis of Crystal Structures. *J. Appl. Crystallogr.* **2006**, *39*, 453–457. <https://doi.org/10.1107/S002188980600731X>.
38. Schmidt, M.W.; Baldrige, K.K.; Boatz, J.A.; Elbert, S.T.; Gordon, M.S.; Jensen, J.H.; Koseki, S.; Matsunaga, N.; Nguyen, K.A.; Su, S.; et al. General Atomic and Molecular Electronic Structure System. *J. Comput. Chem.* **1993**, *14*, 1347–1363. <https://doi.org/10.1002/jcc.540141112>.
39. Yanai, T.; Tew, D.P.; Handy, N.C. A New Hybrid Exchange–Correlation Functional Using the Coulomb-Attenuating Method (CAM-B3LYP). *Chem. Phys. Lett.* **2004**, *393*, 51–57. <https://doi.org/10.1016/j.cplett.2004.06.011>.
40. Etter, M.C.; MacDonald, J.C.; Bernstein, J. Graph-Set Analysis of Hydrogen-Bond Patterns in Organic Crystals. *Acta Crystallogr. Sect. B* **1990**, *46*, 256–262. <https://doi.org/10.1107/S0108768189012929>.
41. Bernstein, J.; Davis, R.E.; Shimoni, L.; Chang, N.-L. Patterns in Hydrogen Bonding: Functionality and Graph Set Analysis in Crystals. *Angew. Chem. Int. Ed.* **1995**, *34*, 1555–1573. <https://doi.org/10.1002/anie.199515551>.
42. Etter, M.C. Encoding and Decoding Hydrogen-Bond Patterns of Organic Compounds. *Acc. Chem. Res.* **1990**, *23*, 120–126. <https://doi.org/10.1021/ar00172a005>.
43. Kennedy, A.R.; Okoth, M.O.; Sheen, D.B.; Sherwood, J.N.; Vrcelj, R.M. Two New Structures of 5-Nitrouracil. *Acta Crystallogr. Sect. C* **1998**, *54*, 547–550. <https://doi.org/10.1107/S0108270197016521>.
44. Srinivasa Gopalan, R.; Kulkarni, G.U.; Rao, C.N.R. An Experimental Charge Density Study of the Effect of the Noncentric Crystal Field on the Molecular Properties of Organic NLO Materials. *ChemPhysChem* **2000**, *1*, 127–135. [https://doi.org/10.1002/1439-7641\(20001103\)1:3<127::AID-CPHC127>3.0.CO;2-1](https://doi.org/10.1002/1439-7641(20001103)1:3<127::AID-CPHC127>3.0.CO;2-1).
45. Koritsansky, T.; Howard, S.; Richter, T.; Mallinson, P.; Su, Z.; Hansen, N. *XD, A Computer Program Package for Multipolar Refinement and Analysis of Charge Density from Diffraction Data*; Free University: Berlin, Germany, 1995.

46. Stewart, J.J.P. MOPAC: A Semiempirical Molecular Orbital Program. *J Comput.-Aided Mol Des.* **1990**, *4*, 1–103. <https://doi.org/10.1007/BF00128336>.
47. Okoth, M.O.; Vrcelj, R.M.; Pitak, M.B.; Sheen, D.B.; Sherwood, J.N. Polymorphism and Hydrated States in 5-Nitrouracil Crystallized from Aqueous Solution. *Cryst. Growth Des.* **2012**, *12*, 5002–5011. <https://doi.org/10.1021/cg300961m>.
48. Craven, B.M. The Crystal Structure of 5-Nitrouracil Monohydrate. *Acta Crystallogr.* **1967**, *23*, 376–383. <https://doi.org/10.1107/S0365110X6700283X>.
49. Pereira Silva, P.S.; Domingos, S.R.; Ramos Silva, M.; Paixão, J.A.; Matos Beja, A. A New Polymorph of 5-Nitrouracil Monohydrate. *Acta Crystallogr. Sect. E* **2008**, *64*, o1091. <https://doi.org/10.1107/S1600536808014426>.
50. Okoth, M.O.; Vrcelj, R.M.; Sheen, D.B.; Sherwood, J.N. Dehydration Mechanism of a Small Molecular Solid: 5-Nitrouracil Hydrate. *CrystEngComm* **2013**, *15*, 8202–8213. <https://doi.org/10.1039/c3ce40749g>.
51. Thomas, R.; Gopalan, R.S.; Kulkarni, G.U.; Rao, C.N.R. Hydrogen Bonding Patterns in the Cocrystals of 5-Nitrouracil with Several Donor and Acceptor Molecules. *Beilstein J. Org. Chem.* **2005**, *15*, 1. <https://doi.org/10.1186/1860-5397-1-15>.
52. Portalone, G. Solid-Phase Molecular Recognition of Cytosine Based on Proton-Transfer Reaction. Part II. Supramolecular Architecture in the Cocrystals of Cytosine and Its 5-Fluoroderivative with 5-Nitrouracil. *Chem. Cent. J.* **2011**, *5*, 51. <https://doi.org/10.1186/1752-153X-5-51>.
53. Portalone, G.; Colapietro, M. An Unusual Syn Conformation of 5-Formyluracil Stabilized by Supramolecular Interactions. *Acta Crystallogr. Sect. C* **2007**, *63*, o650–o654. <https://doi.org/10.1107/S0108270107045659>.
54. Domingos, S.R.; Silva, P.S.P.; Buma, W.J.; Garcia, M.H.; Lopes, N.C.; Paixão, J.A.; Silva, M.R.; Woutersen, S. Amplification of the Linear and Nonlinear Optical Response of a Chiral Molecular Crystal. *J. Chem. Phys.* **2012**, *136*, 134501. <https://doi.org/10.1063/1.3697842>.
55. Petrosyan, A.M.; Giester, G.; Ghazaryan, V.v.; Bezhanova, L.S.; Fleck, M.; Atanesyan, A.K. New Triclinic Polymorph of L-Histidinium 5-Nitrouracilate. *J. Mol. Struct.* **2018**, *1173*, 770–775. <https://doi.org/10.1016/j.molstruc.2018.07.048>.
56. Ramos Silva, M.; Silva, P.; Beja, A.; Paixão, J. Crystal Chemistry of an Atropisomer: Conformation, Chirality, Aromaticity and Intermolecular Interactions. In *Chemical Crystallography*; Connelly, B., Ed.; Nova Science Publishers: New York, NY, USA, 2010; pp. 103–130.
57. Pereira Silva, P.S.; Domingos, S.R.; Ramos Silva, M.; Paixão, J.A.; Matos Beja, A. N,N',N''-Triphenylguanidinium 5-Nitro-2,4-dioxo-1,2,3,4-tetrahydropyrimidin-1-ide. *Acta Crystallogr. Sect. E* **2008**, *64*, o1082–o1083. <https://doi.org/10.1107/S1600536808014244>.
58. Grothe, E.; Meekes, H.; Vlieg, E.; ter Horst, J.H.; de Gelder, R. Solvates, Salts, and Cocrystals: A Proposal for a Feasible Classification System. *Cryst. Growth Des.* **2016**, *16*, 3237–3243. <https://doi.org/10.1021/acs.cgd.6b00200>.
59. Portalone, G. Supramolecular Association in Proton-Transfer Adducts Containing Benzamidinium Cations. I. Four Molecular Salts with Uracil Derivatives. *Acta Crystallogr. Sect. C* **2010**, *66*, o295–o301. <https://doi.org/10.1107/S0108270110016252>.

Disclaimer/Publisher's Note: The statements, opinions and data contained in all publications are solely those of the individual author(s) and contributor(s) and not of MDPI and/or the editor(s). MDPI and/or the editor(s) disclaim responsibility for any injury to people or property resulting from any ideas, methods, instructions or products referred to in the content.